Fuzzy-controlled individual-cell equaliser using discontinuous inductor current-mode Cûk convertor for lithium–ion chemistries

Yuang-Shung Lee and Jiun-Yi Duh

Abstract: An intelligent battery equalisation-scheme based on fuzzy-logic control (FLC) is presented to adaptively control the equalising process for series-connected lithium–ion batteries. The proposed individual-cell equalisation scheme (ICE) is a bidirectional DC–DC convertor based on the Cûk convertor operated in the discontinuous inductor current mode (DICM). The proposed method can be used to achieve a zero-current-switching (ZCS) cell-balancing control scheme to reduce the switching losses in MOSFET switches. Further, a fuzzy-logic-controlled strategy is constructed with a set of membership functions to prescribe the cell equalising behaviour within a safe equalising region for reduced cell-equalisation time. The simulation and experimental results show the advantage of the predicted equalising performance for lithium–ion battery stacks. The proposed fuzzy-logic-control battery-equalisation controller (FLC-BEC) abridges the equalisation time by about 30% compared with the equaliser without FLC. The power losses of the MOSFET switch are significantly reduced by about 33.8%, and the equalisation efficiency is increased by about 8.5% compared with the same equalisation scheme in continuous-inductor-current mode (CICM). The proposed equalisation method maintains safe operations during the charge/discharge state to increase the charge capacity of lithium–ion battery-pack cells.

1 Introduction

The power-rate density for lithium–ion batteries is triple that for lead-acid batteries and one-and-a-half times that for alkaline batteries, such that lithium–ion batteries have successfully become a significant chargeable-battery source for computers, communications and consumer-electronic products with numerous high-technology industry applications [1]. Because the voltage in a single battery cell is inherently low, battery cells connected in series are usually employed in many practical applications such as electric vehicles (EV), hybrid electric vehicles (HEV), electric scooters (ES) and consumer electronics. Imbalanced cell voltage within a series string can be attributed to the differences in cell internal resistance, unbalanced state of charge (SOC) between cells, degradation and the ambient-temperature gradients of the battery pack during charging and discharging. Voltage-monitoring and current-diverting equalisation circuits and battery-management systems (BMS) have been presented in the literature to prevent imbalances during charging and discharging in series-connected battery cells [2, 3].

Integrated individual cell equalisation schemes (ICE) for battery-pack applications have been proposed to equalise battery strings [2–5]. The bidirectional battery-equalisation scheme has many advantages such as higher equalisation efficiency for nondissipative current diverters and a modular design approach [2]. The disadvantage of this equalisation scheme is that the stored energy in the inductor is transferred only to the weaker cell in the $(1-D)T_s$ duty cycle. The equalisation time and efficiency of this equalisation scheme are therefore poor for practical battery-equalisation applications in the smart-battery-management system (SBMS) [6].

Battery-equalisation control should be implemented to restrict the charge–discharge current to the allowable cell limitations in the battery string. Lithium–ion-battery chemistries cannot withstand overcharge in the charging state. An overcharge will vaporise the active materials in the battery, increase the internal pressure and produce a higher risk for explosion [4, 5]. During discharge, lithium–ion batteries must be prevented from being excessively discharged to the low-voltage limit [5]. Overdischarge will dissolve the copper in the electrolyte and form copper dendrites that harm the battery and shorten the battery-cell life. Series-connected lithium–ion batteries present a more complex problem; therefore, careful monitoring and controls must be considered to avoid any single cell from experiencing overvoltage or undervoltage from excessive charging and discharging. Because a lithium–ion battery must not be overcharged and overdischarged, ICE must be employed to prevent, diagnose and correct any cell-voltage imbalance in a lithium–ion-battery string [6]. Cell-balancing control is designed to obtain the maximum usable capacity from the lithium–ion battery string. Because battery-string charging and discharging are limited by any single cell reaching its end-of-charge voltage (about 4.1–4.2 V/cell) and low-voltage threshold (about 2.0–2.5 V/cell), cell-balancing algorithms search to remove energy efficiently from a strong cell and transfer that energy into a weak cell until the cell voltage is equalised to the same level across all cells. This enables additional charging capacity to be achieved for the entire battery string [4].

IEE Proceedings online no. 20050017

doi:10.1049/ip-epa:20050017

Paper first received 20th January and in final revised form 18th April 2005

The authors are with the Department of Electronic Engineering, Fu-Jen Catholic University, 510 Chung-Cheng Road, Hsin-Chuang, Taipei 24205, Taiwan

E-mail: lee@ee.fju.edu.tw

The serious cell-voltage imbalance in the battery string usually generates because of changes in the internal impedance and/or cell capacity shrinking due to ageing. Charged and discharged excursions to these cells will shrink the capacity and/or high internal impedance will produce large voltage swings. During lithium–ion-battery applications in highly transient regenerative braking in EV or HEV, the inrush of instantaneous regenerative-braking current will generate a sudden voltage, increasing in the lithium–ion battery, and exceed the electrolyte breakdown threshold. It is necessary to balance the lithium-cell chemistries because of these transient-overvoltage situations. Therefore, cell-balancing algorithms must respond quickly and adaptively to regulate the performance for the desired battery dynamic system. Another significant consideration is the time required to execute a cell-voltage-balancing algorithm. Typical equalising current is about C/100 ~ C/50 or under 100–300 m A for most applications if viewed as the top-off phase to the charging algorithm. This is not acceptable in fast-charging algorithms and quick-response battery-management-control systems [5]. Therefore, developing a fast-response cell-balancing control technology and intelligent algorithm for the smart-battery-management system is a significant issue in lithium-based battery applications [5, 6].

To observe the charged and discharged characteristics of the lithium–ion battery, the energy efficiency of the charge/discharge is also affected by the temperature gradients of the battery pack, impedance and usable capacity of each cell, and the duration of the cell-voltage-balancing control process. Prediction of these battery-equalisation control factors is very complicated. By application of the fuzzy-logic-control (FLC) method, the control factors can be reduced. The FLC method is proper for predicting the nonlinear behaviour of battery equalisation because it has more adaptability, robustness and better efficiency for nonlinear control systems. A fuzzy-logic-controlled battery-equalisation controller (FLC-BEC) is employed to regulate

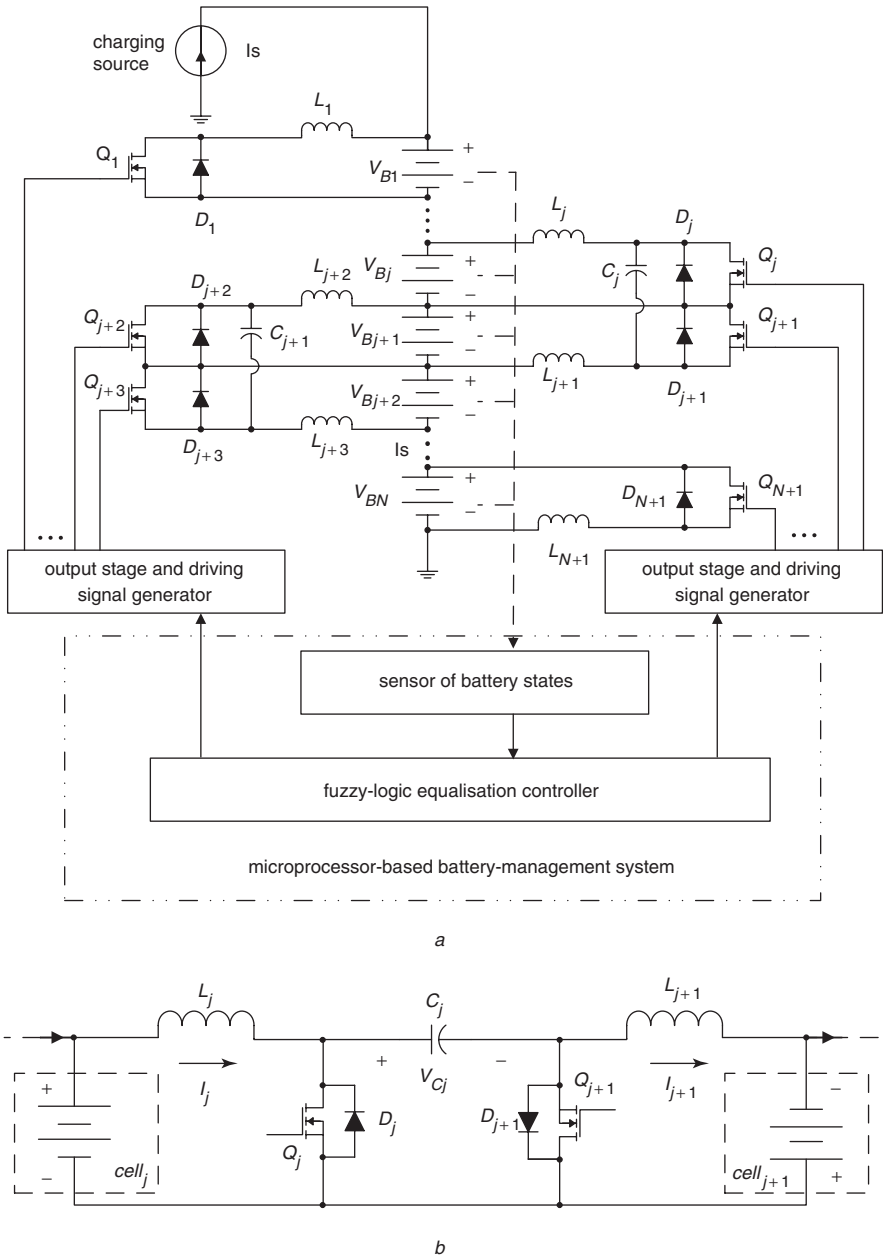

Fig. 1 *Charging system with ICE and BMS*
a Configuration
b Proposed ICE

the equalising current of the proposed equalisation scheme. The rule base collects the control rules that describe the knowledge and experience of the battery-equalisation control in the fuzzy set. A complicated and unpredictable mathematical model of the battery cell is not required to describe the cell-balancing system in the FLC design method [7, 8].

Complete cell-voltage balancing is performed using a bidirectional DC–DC convertor based on the Cûk convertor [9]. This unit can be designed to operate in the discontinuous-inductor current mode (DICM) to obtain zero-current switching in MOSFET switches [10]. Because DICM operation will restrict the average equalisation current during the battery-equalisation process, the battery-equaliser response will be reduced. Therefore, an intelligent controller is needed to compensate the equaliser performance. In the conventional controller-design approach, it is difficult to construct the battery-cell model that describes the equalisation characteristics of lithium–ion battery strings because of the inherent uncertainty in the electrochemical reactions [7, 8]. The derived FLC-BEC signals correspond to the respective cell-voltage and cell-voltage differences in the battery string. The bidirectional nondispative cell-voltage-equalisation scheme with FLC-BEC allows dynamic equalisation between cells during both charging and discharging. A design example for the series-connected lithium–ion-battery string was constructed to achieve the predicted equalising performance. The proposed FLC-BEC can reduce the equalisation time and maintain safe operations for each lithium–ion cell in the battery string during the charge/discharge state. The efficiency of the battery pack is improved by the intelligent battery equalisation design.

2 Proposed individual cell equaliser

The studied battery-charging system with the proposed ICEs and the microprocessor based BMS is shown in Fig. 1*a*. The system is composed of N battery cells, $(N-1)$ ICEs, $2(N-1)$ inductors and MOSFET switches. The jth module is comprised of two inductors L_j and L_{j+1}, an energy-transfer capacitor C_j, and two power MOSFETs with body diodes as the battery cell-balancing switches. This system is redrawn and simplified in Fig. 1*b*. The cell-voltage-balancing control algorithm for this equalisation scheme is instructed by a microprocessor-based BMS. The energy between the adjoining battery cells is transformed through the energy-transfer capacitor. The energy-transfer direction is determined by the cell voltage and/or SOC difference in the battery string and conduction from the controlled power-MOSFET switches [9]. The two adjoining cells are balanced by switching the MOSFETs on/off according to the PWM signals generated from the BMS. The PWM signals correspond to the respective cell voltage through the microprocessor-based BMS, which controls the switches Q_j and Q_{j+1}. The initial capacitor voltage V_{C_j} equals $V_{B_j} + V_{B_{j+1}}$. For example, the PWM control signal turns on/off the Q_j to transfer some of the stronger cell voltage V_{B_j} to the weak cell $V_{B_{j+1}}$. The stronger cell energy is transferred from cell V_{B_j} to cell $V_{B_{j+1}}$. Conversely, if cell $V_{B_{j+1}}$ is stronger than the weaker cell V_{B_j}, the energy is transferred from cell $V_{B_{j+1}}$ to cell V_{B_j} by controlling the Q_{j+1}. The equalisation process will be uninterrupted until the voltages in the remaining cells are all equalised to the same level.

For simplicity of steady-state analysis, assume that the voltage V_{C_j} is constant because the selected capacitance is adequate [10]. Using the voltage second balance across L_j and L_{j+1} over one time period in the boundary condition between CICM and DICM, the voltage and current transfer ratio of the jth ICE can be obtained as

$$\frac{V_{B_{j+1}}}{V_{B_j}} = \frac{I_j}{I_{j+1}} = \frac{D}{1-D} \tag{1}$$

where D is the duty ratio of the convertor switches. From

$$e = L\frac{di}{dt}$$

the peak inductor currents are: $i_{j+1\,peak} = V_{B_{j+1}}(1-D)T_S/L_{j+1}$ and $i_{jpeak} = (1-D)\cdot V_{B_{j+1}}T_S/L_j$. Because the average equalisation current is $I_k = \frac{1}{2}i_{kpeak}$, the boundary conditions for operating in discontinuous-inductor-current mode (DICM) can be expressed using the two equations [11]

$$T_S \geq \frac{2L_{j+1}I_{j+1}}{(1-D)V_{B_{j+1}}} \tag{2}$$

$$T_S \geq \frac{2DL_jI_{j+1}}{(1-D)^2V_{B_{j+1}}} \tag{3}$$

where $T_s = 1/f_{sw}$ and f_{sw} is the switching frequency of the convertor. Eqns. (2) and (3) are the boundary conditions for the proposed battery-equalisation scheme to differentiate between CICM and DICM [4, 10]. The equivalent circuit

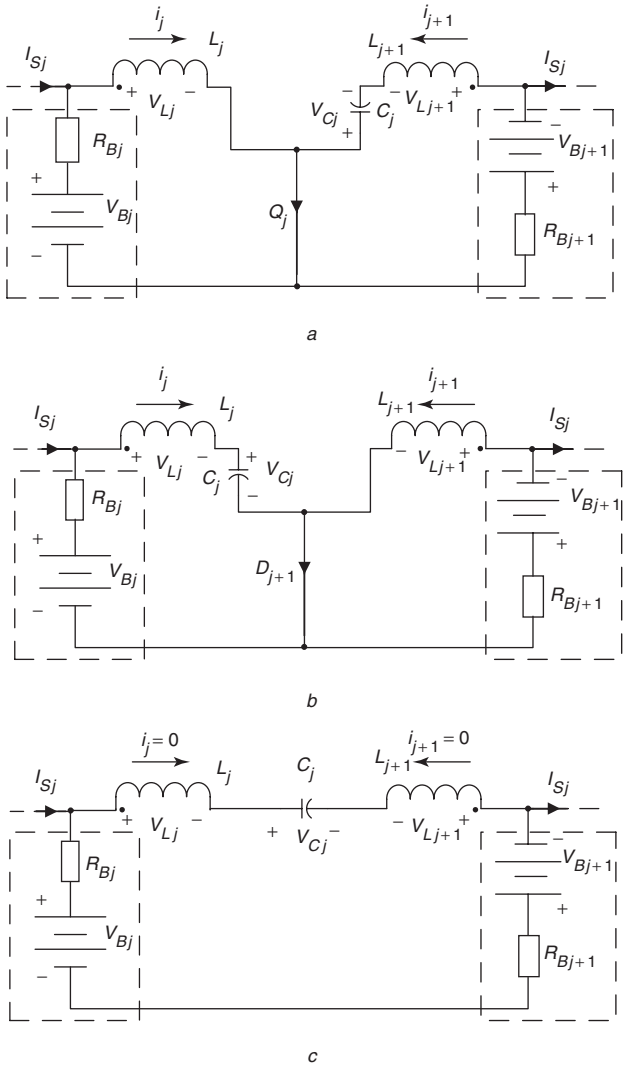

Fig. 2 *Equivalent circuit of DICM for* $V_{B_j} > V_{B_{j+1}}$
a t_0–t_1, Q_j turn-on
b t_1–t_2, D_{j+1} turn-on
c t_3–t_4, Q_j and D_{j+1} all turn-off

for $V_{B_j} > V_{B_{j+1}}$ in the DICM is showed in Fig. 2 and analysed as follows:

[*Stage 1.* (Fig. 2*a*: $t_0 < t < t_1$)]: The MOSFET Q_j is turned on and the diode D_{j+1} is turned off. The switching variable is $u = 1$ and $u^* = 0$. The energy stored in the capacitor is charged to the weak cell $V_{B_{j+1}}$. The dynamic equations are

$$L_j \frac{di_j}{dt} = V_{B_j} - (I_{sj} - i_j)R_{B_j},\ i_j(t_0) = I_0 \tag{4}$$

$$L_{j+1} \frac{di_{j+1}}{dt} = -V_{B_{j+1}} - (I_{sj} + i_{j+1})R_{B_{j+1}} + V_{C_j},\ i_{j+1}(t_0) = I_0 \tag{5}$$

$$C_j \frac{dV_{C_j}}{dt} = -i_{j+1},\ V_{cj}(t_0) \cong V_{B_j} + V_{B_{j+1}} \tag{6}$$

where the initial current I_0 is zero when operating in the DICM. I_{sj} is composed of the charging current and the equalising current for the other ICE cell. R_{B_k} is the equivalent series resistance (ESR) of the kth battery cell.

[*Stage 2.* (Fig. 2*b*: $t_1 < t < t_2$)]: For this interval, MOSFET Q_j is turned off and the diode D_{j+1} is forced to turn on. The switching variable is $u = 0$ and $u^* = 0$. The energy stored in the capacitor recharges to the weak cell $V_{B_{j+1}}$. The dynamic equations are:

$$L_j \frac{di_j}{dt} = V_{B_j} - (I_{sj} - i_j)R_{B_j} - V_{C_j},\ i_j(t_1) = I_p \tag{7}$$

$$L_{j+1} \frac{di_{j+1}}{dt} = -V_{B_{j+1}} - (I_{sj} + i_{j+1})R_{B_{j+1}},\ i_{j+1}(t_1) = I_p \tag{8}$$

$$C_j \frac{dV_{C_j}}{dt} = i_j,\ V_{cj}(t_1) \cong V_{B_j} + V_{B_{j+1}} \tag{9}$$

[*Stage 3.* (Fig. 2*c*: $t_2 < t < t_3$)]: The MOSFET Q_j and the diode D_{j+1} are both turned off, the switching variable $u^* = 1$ and $u =$ floating state; therefore, the inductor currents are zero when V_{C_j} is charged to $V_{B_j} + V_{B_{j+1}}$, and $\frac{di_j}{dt} = \frac{di_{j+1}}{dt} = \frac{dV_{C_j}}{dt} = 0$. The voltage-balance equation is

$$V_{B_j} + V_{B_{j+1}} + I_{Sj}(R_{B_j} + R_{B_{j+1}}) = V_{C_j} \tag{10}$$

Based on the above, the system can be represented using the following state equation in which $u = 1$ and $u^* = 0$ when Q_j is turned on and D_{j+1} is turned off, $u = 0$ and $u^* = 0$ when Q_j is turned off and D_{j+1} is forced to turn on, $u^* = 1$ and $u =$ floating state when Q_j and D_{j+1} are both turned off:

$$\dot{x} = Ax + bI_{Sj} + \zeta \tag{11}$$

$$\text{where } A = \begin{bmatrix} \frac{R_{B_j}}{L_j} & 0 & \frac{-(1-u)}{L_j} \\ 0 & -\frac{R_{B_{j+1}}}{L_{j+1}} & \frac{u}{L_{j+1}} \\ \frac{1-u}{C_j} & \frac{-u}{C_j} & -u^* \end{bmatrix}$$

$$b = \begin{bmatrix} -\frac{R_{B_j}}{L_j} \\ -\frac{R_{B_{j+1}}}{L_{j+1}} \\ (R_{B_j} + R_{B_{j+1}})u^* \end{bmatrix}$$

$$\zeta = \begin{bmatrix} \frac{V_{B_j}}{L_j} \\ -\frac{V_{B_{j+1}}}{L_{j+1}} \\ (V_{B_j} + V_{B_{j+1}})u^* \end{bmatrix}$$

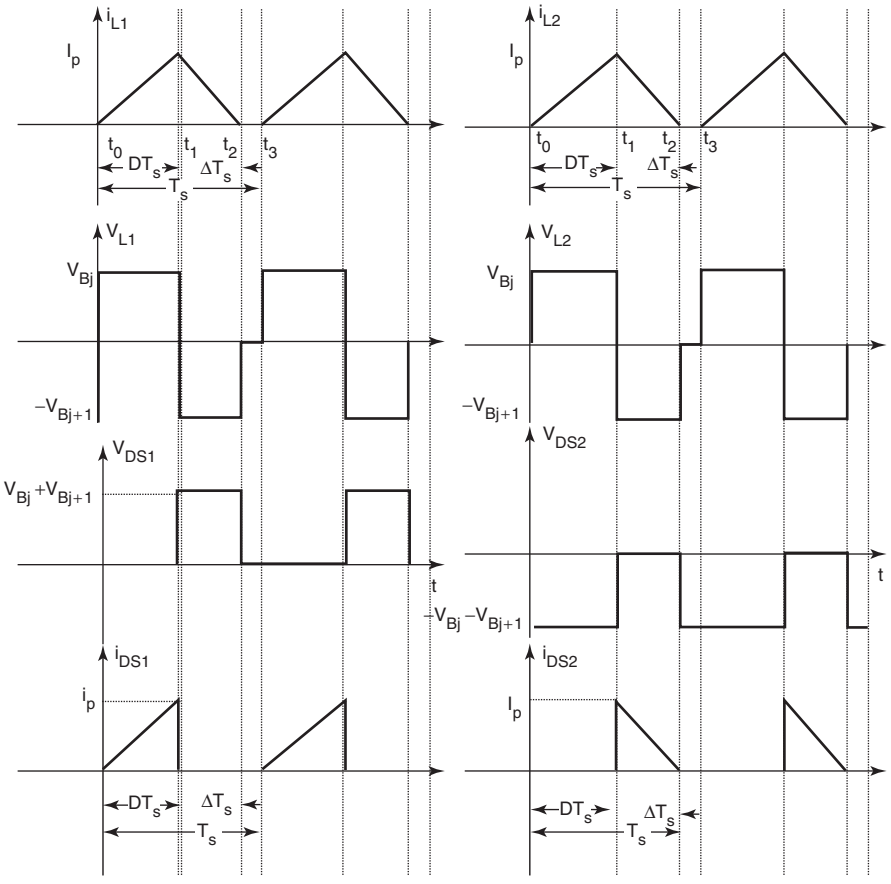

Fig. 3 *Typical switching waveforms of ICE for* $V_{B_j} > V_{B_{j+1}}$

$$\dot{x} = \left[\frac{di_j}{dt}, \frac{di_{j+1}}{dt}, \frac{dV_{C_j}}{dt}\right]^T$$
$$x = \left[i_j, i_{j+1}, V_{C_j}\right]^T$$
$$j = 1, 2, 3, \ldots, N \text{ for } V_{B_j} > V_{B_{j+1}}$$

and I_{Sj} contains a parameter used to control the battery-charge current. u is a PWM control signal of MOSFET used to equalise the cell voltage of the battery string.

Neglecting the effects of the charging current, Fig. 3 shows the typical switching waveforms for the proposed ICE operated in the DICM. The equivalent series resistance (ESR) of the lithium–ion battery R_B is very low (about $0.001 \sim 0.002\,\Omega$). The voltage drop at this resistor is neglected in the analysis and convertor design; therefore the equalising current of the proposed ICE is dependent only on the command generated from the BMS-equalisation algorithm. The charging-current source I_s will not affect the equalisation current but can increase or decrease the battery current during the charged or discharged states. If $V_{B_j} > V_{B_{j+1}}$, the equalising current flows through L_j and L_{j+1} in the same phase. Similarily, if $V_{B_j} < V_{B_{j+1}}$, the current flows through L_j and L_{j+1} in the opposite direction but still in the same phase. The system state equation has a bilinear relationship compared with (11). The state–space equation of the proposed bidirectional battery equaliser in both conditions for $V_{B_j} > V_{B_{j+1}}$ or $V_{B_j} < V_{B_{j+1}}$ can be obtained as follows [9]:

$$\dot{x} = \Gamma x + \mathbf{B} I_{Sj} + \xi \tag{12}$$

where

$$\Gamma = \begin{bmatrix} \text{sgn}\dfrac{R_{B_j}}{L_j} & 0 & \dfrac{-(1-u)}{L_j} \\ 0 & -\text{sgn}\dfrac{R_{B_{j+1}}}{L_{j+1}} & \dfrac{u}{L_{j+1}} \\ \dfrac{1-u}{C_j} & \dfrac{-u}{C_j} & -u^* \end{bmatrix},$$

$$B = \begin{bmatrix} -\text{sgn}\dfrac{R_{B_j}}{L_j} \\ -\text{sgn}\dfrac{R_{B_{j+1}}}{L_{j+1}} \\ (R_{B_j} + R_{B_{j+1}})u^* \end{bmatrix},$$

$$\xi = \begin{bmatrix} \text{sgn}\dfrac{V_{B_j}}{L_j} \\ -\text{sgn}\dfrac{V_{B_{j+1}}}{L_{j+1}} \\ (V_{B_j} + V_{B_{j+1}})u^* \end{bmatrix},$$

and $x = [i_j, i_{j+1}, V_{Ci}]^T$, $\text{sgn} = \text{sign}(V_{B_j} - V_{B_{j+1}})$, and $j = 1, 2, \ldots, N$.

The voltage and current-transfer ratio of the jth ICE operating at DICM can be obtained as

$$\frac{V_{B_{j+1}}}{V_{B_j}} = \frac{I_{L_j}}{I_{L_{j+1}}} = \frac{D}{\Delta}$$

The average current for the inductor I_{L_k} is

$$I_{L_k} = \frac{V_{C_j} V_{B_k} D^2 T_S}{2L_k(V_{C_j} - V_{B_k})} \tag{13}$$

where $k = j$ or $j+1$ and T_s is the switching period for the battery equaliser.

The proposed ICE is designed in the DICM by selecting the appropriate switching duty as required for obtained ZCS soft-switching effects, since the ICE is designed to operate in DICM and the average equalising current is small. Therefore, we need an intelligent control algorithm to improve the cell equaliser's dynamic performance. When the difference in the cell voltage is great, the equalisation time becomes too long for quick BMS response. The FLC-BEC is employed to speed up and monitor the equalisation process.

3 FLC-BEC design

The battery-pack system uses an intelligent approach to control cell equalisation. The FLC consists of the rule base, inference engine, fuzzification and defuzzification, as shown in Fig. 4. There are two inputs in the FLC. Each input is the voltage difference V_d between two cells and the cell voltage V_B in the battery strings. The numerical inputs are converted into linguistic fuzzy sets by the fuzzifier. The linguistic control values are generated in the inference engine based on the input fuzzy values and the preconstructed rule base. The linguistic inference results are converted into numerical output I_{BEC} by the defuzzifier. The fuzzy controlled output I_{BEC} is the desired battery-equalising current of the proposed cell-equalisation scheme. To maintain battery-string dynamic equalisation within a safe region for the voltage specification, the allowable balancing-voltage-interval limitation for the MRL/ITRI 10 Ah lithium–ion battery is defined between 2.8 (V) and 4.1 (V).

Figure 5 shows the three membership-function sets for the equalising strategy in the proposed FLC-BEC that is the voltage-different-sense fuzzy variable μ_A with respect to V_d, and the cell-voltage-sense fuzzy variable μ_B with respect to V_B, and the output fuzzy variable μ_0 with respect to the battery-equalizing current I_{BEC}. Five membership functions are adopted: very large (VL), large (L), medium (M), small (S) and very small (VS) to describe the fuzzy sets. These functions are all described using the same five linguistic variables.

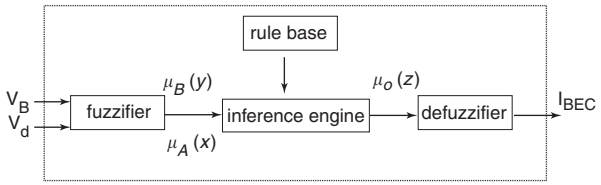

Fig. 4 *Block diagram of the FLC*

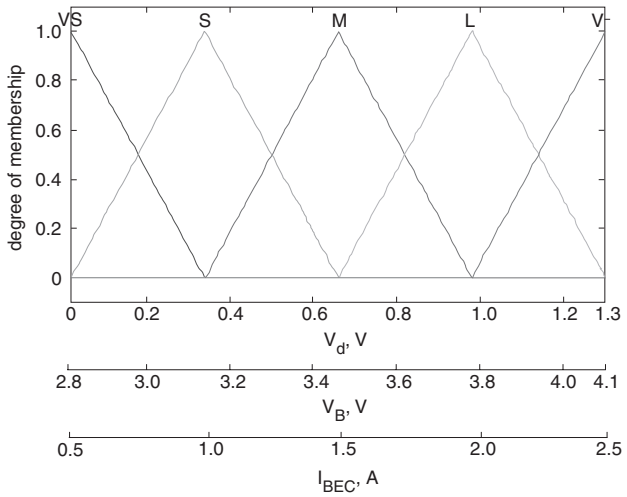

Fig. 5 *FLC-BEC membership function with respect to $\mu_A(x)$, $\mu_B(y)$ and $\mu_o(z)$*

The fuzzy-rule base for the control system was set according to professional experience with cell-balancing control systems. The consideration and experience for the cell-balancing control system of a lithium–ion battery string are summarised as follows:

(i) The equalisation algorithm will be started when the voltage difference between two adjoining cells exceeds 0.0196 (V) (hardware resolution limit of ADC0804) to minimise the cell-to-cell imbalance.

(ii) During the charge-equalisation state, the cell voltage cannot exceed its end-of-charge voltage (about 4.1 V/cell) to prevent overcharging and dissolving the copper in electrolyte, with damage to the active materials.

(iii) During the discharged equalisation state, the cell voltage cannot go below its low-voltage threshold (about 2.8 V/cell) to prevent overdischarge and damaging to the cell capacity and life.

(iv) When the voltage difference between adjoining cells is large, a higher equalisation current is needed to speed up the time required to execute a balancing algorithm.

(v) When the voltage difference between adjoining cells is small, a small equalisation current is needed to prevent low-voltage cell overdischarge.

(vi) If either a cell voltage in the battery string exceeds its end-of-charge voltage during charge-equalisation state, or one cell voltage in the battery string reaches its low-voltage threshold during discharge equalisation, the BMS will send a command to stop the cell-voltage-balancing process.

Table 1: Control-rule base of FLC-BEC for linguistic variables

Cell voltage, V_B	Voltage difference, V_d				
Output	*VS*	*S*	*M*	*L*	*VL*
VS	*VS*	*M*	*L*	*VL*	VL[1]
S	*VS*	*M*	L[3]	VL[2]	*VL*
M	*VS*	M[6]	L[5]	VL[4]	*VL*
L	[12] VS [9]	S[8]	M[7]	*L*	*VL*
VL	[13] VS [11]	S[10]	*M*	*L*	*VL*

Based on the cell-balancing control strategies in this battery-equalisation technology, the fuzzy-control rules for the FLC-BEC in the battery-equalisation scheme are presented as follows:

$$R^{\ell}: \text{IF } v_d^{\ell} \text{ is } LGSV_d^{\ell} \text{ and } v_B^{\ell} \text{ is } LGSV_B^{\ell} \text{ THEN } I_{BEC}^{\ell} \text{ is } LGSI_B^{\ell}$$

where *LGSV* and *LGSI* are the linguistic values for the general signed disturbance in the ℓth variable for the input and output fuzzy sets.

The rule base collects the control rules that describe the knowledge and experience of the battery-equalisation control in the fuzzy set. The decision-rule table for the linguistic variables for the FLC is two-dimensional (5×5) and is constructed in the intelligent-control-scheme rule-based memory system, shown in Table 1. The fuzzy inference engine is an intelligent operating algorithm that transforms the fuzzy-rule base into fuzzy linguistic output. The linguistic inference results are converted into numerical output I_{BEC} by the defuzzifier. The fuzzy controlled output I_{BEC} is the desired battery-equalising current for the proposed cell-equalisation scheme.

A state–space approach is adopted to inspect the stability of the proposed FLC-BEC [12]. Stability analysis of a conventional FLC requires characterisation of the relation between the relative influence of each rule of the rule base and the control action of the dynamic system. The closed-loop system trajectory mapped on the partition space of the fuzzy-rule table is also shown in Table 1, and the grey cells show the fired rule according to the specified equalisation control action of the battery string. The linguistic trajectory corresponds to the proposed system trajectory associated with the cell-volatge-balancing trajectory in Table 1, i.e.

$$\begin{aligned}\text{Linguistic trajectory} = (&\text{Rule1}, \text{Rule2}, \text{Rule3}, \text{Rule4}, \text{Rule5},\\ &\text{Rule6}, \text{Rule7}, \text{Rule8}, \text{Rule9}, \text{Rule10},\\ &\text{Rule11}, \text{Rule12}, \text{Rule13})\end{aligned}$$

Rule1 is the fuzzy rule starting at a very large (VL) voltage difference, a very small (VS) cell voltage and a very large (VL) output. Through the control action of the FLC, the trajectory reaches Rule13, which is the control goal of the FLC-BEC. This denotes that the system trajectory has reached the desired goal and terminated at a very small (VS) voltage difference, a very large (VL) cell voltage and a very

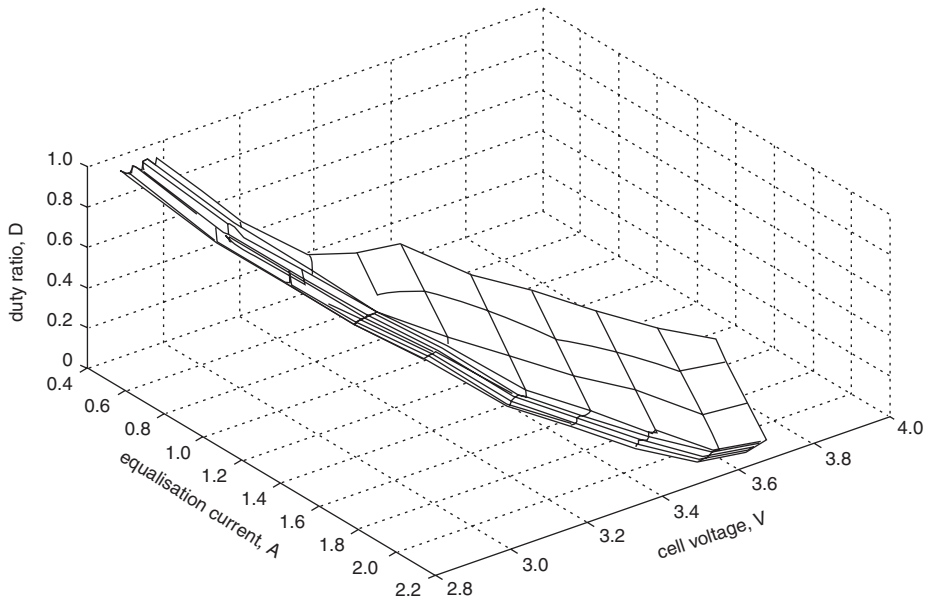

Fig. 6 *Switching surface of the proposed FLC-BEC*

small (VS) output. The corresponding control error of the cell voltages is plotted in Fig. 10. These errors converge to zero in the final state of the dynamic trajectory. From the observation of Table 1 and Fig. 10, the controlled system with the proposed FLC-BEC is stable [12].

The nominal operating point of the proposed equaliser is designed in DICM with a duty of 0.5. However, in the FLC, the equalising current is a controlled variable according to the system desired. Figure 6 shows the corresponding duty ratio (D) with respect to the measured cell voltage and the equalisation current of the ICE with FLC-BEC lying in the switching surface that is calculated from (3) for the system being studied. The switching surface of the designed FLC is under the boundary between DICM and CICM. Thus, the operating mode of the proposed ICE with FLC-BEC is always working at DICM in this designed case for the value of ZCS obtained to reduce the switching loss. The systematic design procedures for the proposed FLC-BEC are summarised as follows:

Step 1: Obtain the true value w_{ij} for the ith input membership function for x and the jth input membership function for y using

$$w_{ij} = \min\{\mu_{Ai}(x), \mu_{B_j}(y)\} \text{ for } i = 1, \ldots, 5 \text{ and } j = 1, \ldots, 5$$

Step 2: Calculate the fuzzy-output value $\mu_{oij}(z)$ using w_{ij} and the kth output membership function according to each rule; $\mu_{ok}(z)$ is

$$\mu_{oij}(z) = \min\{\omega_{ij}, \mu_{ok}(z)\} \text{ for } k = 1, \ldots, 5$$

Step 3: Determine the fuzzy set for output z,

$$\mu_{out}(z) = \max\{\mu_{o11}(z), \mu_{o12}(z), \ldots, \mu_{o54}(z), \mu_{o55}(z)\}$$

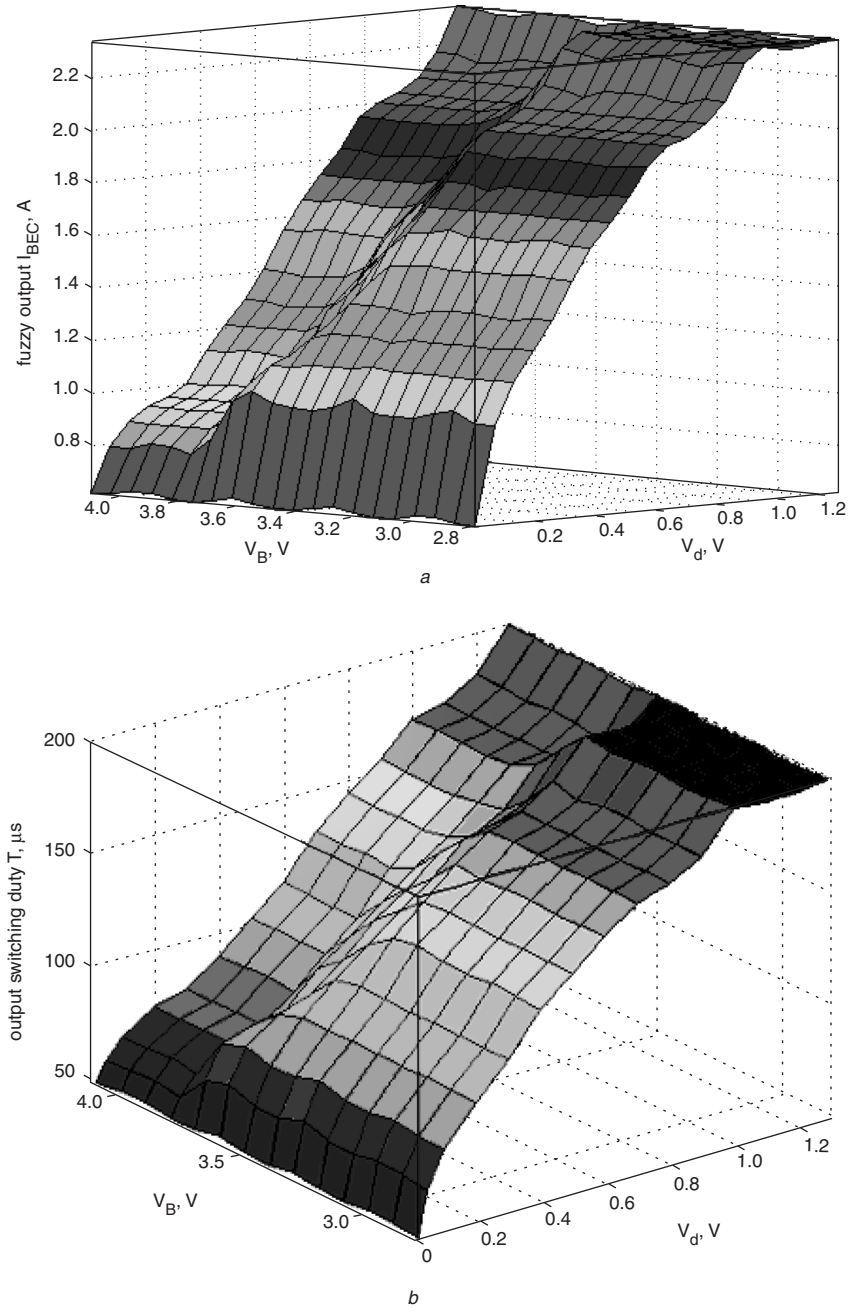

Fig. 7 *FLC output*
a I_{BEC} against V_d and V_B
b T_s against V_d and V_B

Step 4: Find the output battery-equalisation current I_{BEC} (A) of the FLC-BEC using the inference results through the defuzzification process using the center-of-gravity approach, expressed as:

$$I_{BEC} = \frac{\sum_{l=1}^{m} \mu_{out}(z_l) \cdot z_l}{\sum_{l=1}^{m} \mu_{out}(z_l)} (\mathrm{A}) \quad (14)$$

Step 5: Transform the output battery-equalising current I_{BEC} (A) into the corresponding switching period of the PWM-driving signal for the proposed battery-equalisation scheme using (13), and rewritten as

$$T_S = \frac{2I_{BEC}L_j(V_{C_j} - V_{B_j})}{D^2 V_{B_j} V_{C_j}} \quad (15)$$

The numerical output I_{BEC}, the designated equalisation current for the battery cell corresponding to V_d and V_B can be determined using the controller-design procedure. The design parameters of the FLC-BEC are: $L_j = 100\,\mu\mathrm{H}$, $D = 0.5$, with the internal resistances of the cells are neglected in the designed case. A three-dimension graphical representation of the fuzzy-logic controller output I_{BEC} with respect to V_d and V_B is depicted in Fig. 7*a*. The corresponding output switching period T_s of the driving signal for the ICE is also plotted in Fig. 7*b*. The switching period is used to regulate the equalisation current for the cell-voltage-balancing control system according to the cell voltage, cell-voltage difference, and the prescribed fuzzy-rule base. Figure 7 shows that the battery-equalising current is adjusted according to the cell-voltage difference and the battery-string cell voltage. The larger cell-voltage difference and the larger cell voltage will enable the FLC inference engine to generate a higher battery-equalising current to balance the adjoining cell voltage in the battery string. To reduce the time required to calculate the FLC-BEC algorithm in a practical hardware implementation, the calculation results from steps 1 to 4 and step 5 are predesigned as a look-up table stored in the memory of the BMS microprocessor. The execution time for the control force determined from the lookup table of the proposed FLC-BEC is very short; shorter than the convertor switching period. Consequently, there is no execution problem in the designed FLC-BEC due to the repetition rate for fuzzy-control-strategy execution. The equalising current is adaptively regulated online according to states of battery-pack measurements, such that the proposed ICE can shorten the equalisation time compared with that for the conventional scheme without FLC. The proposed FLC-BEC can speed up the battery-equalising processing and monitor the cell voltage of a lithium–ion battery within a safety region during the equalisation process.

4 Simulation and experiments

To verify the results, a PSpice simulation was performed for a three-module battery stack with two proposed equalisers, ICE1 and ICE2, as shown in Fig. 8. For simplicity, the battery storage elements were assumed to be capacitors that have been established in the library of the simulation package by using a capacitor with an ESR. The battery initial voltages in the simulations were set to $V_{B1} = 3.95$ (V), $V_{B2} = 3.81$ (V) and $V_{B3} = 3.2$ (V). The energy-storage-element capacitance was selected as 5 mF with ESR = $0.001\,\Omega$. The circuit parameters were $L_1 \sim L_4 = 100\,\mu\mathrm{H}$, and $C_1 = C_2 = 470\,\mu\mathrm{F}$. The battery-equalisation system was driven using a nominal switching frequency of 16.67 kHz with duty $D = 0.5$ for both $V_{B1} > V_{B2} > V_{B3}$ and $V_{B1} < V_{B2} < V_{B3}$ to ensure that the proposed ICE operated at the DICM that could obtain a zero-switching transient to decrease the MOSFET switching loss. Figure 9*a* and *b* shows the simulating inductor currents and the corresponding voltages for $V_{B1} > V_{B2} > V_{B3}$ and $V_{B1} < V_{B2} < V_{B3}$, respectively. The cell-balancing-control processing stops until the cell voltages are equalised to the same end-of-charge state. The capacitance in practical simulation is chosen to be much smaller than the theoretical value of the battery cell for stabilising and speeding the simulation process. Therefore, the equalisation time in a simulation for reaching the same end-of-charge/discharge is shorter than the experimental result.

A three-module battery stack with two proposed ICE was installed for the experiment which was used to verify

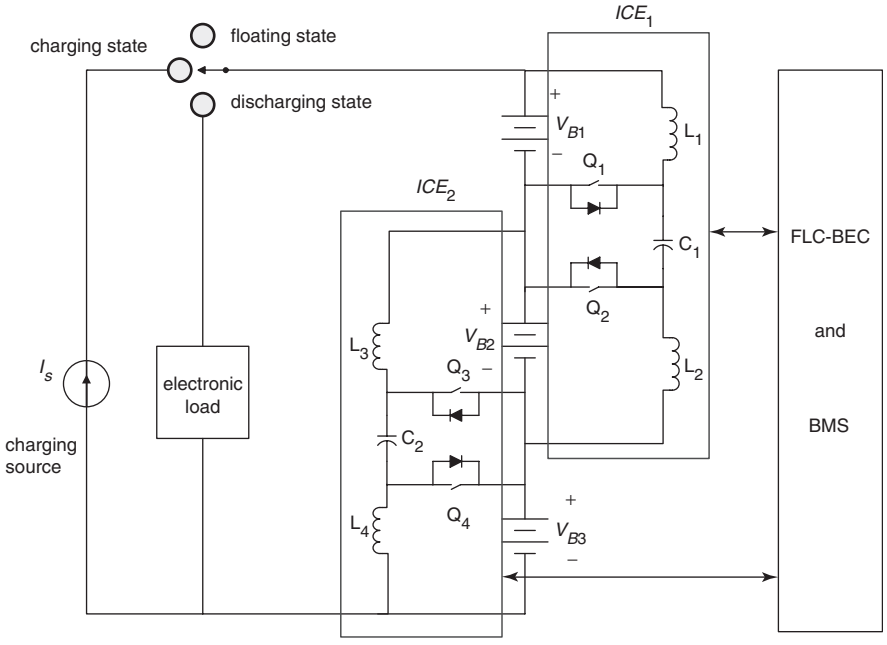

Fig. 8 *Experimental set-up*

the performance of the proposed equaliser. The driving signals for the two equalisation schemes were controlled using a BMS according to the sensed cell states. The driving signals were constructed using a logical switching algorithm and the intelligent BMS-algorithm decision strategy instructed using an 8052 microprocessor. The battery stacks were MRL/ITRI-10 Ah lithium–ion batteries with the same initial voltages. The parameters were $L_1 = 98.1\,\mu H$, $L_2 = 101.3\,\mu H$, $L_3 = 103.0\,\mu H$, $L_4 = 99.4\,\mu H$, and $C_1 = C_2 = 470\,\mu F$. The ICE was driven using a 16.67 kHz switching frequency with a duty $D = 0.5$ for nominal operating condition. The inductor currents and voltages are shown in Fig. 9*b* and *d*, respectively. The experimental results were the same as the theoretical analysis and simulations. During the DICM, the MOSFETs are turned on at zero current state and the body diodes are also turned off at zero current state; therefore, the power losses of the main switches can be reduced compared with those designed in CICM. Figure 11 shows the measured power losses of the MOSFET switch, $P_T = V_T i_T$ and the corresponding FFT frequency spectrums of the proposed battery equaliser under the CICM ($D = 0.53$) and DICM ($D = 0.5$), respectively. It clearly shows that the DC component and the low-order harmonic are high when the ICE operated in CICM. The high-frequency harmonics in the proposed equaliser operated in DICM are weaker than that is designed in CICM. The experimental results of the equalisation efficiency of ICE under various operating modes for the specified equalisation processing are shown in Fig. 11*e*. The MOSFET switches of the proposed battery equaliser are turned off in the zero current state. The power losses of the MOSFET switch in the battery equaliser can be reduced significantly, by 33.8%, compared with the same equaliser operated in CICM. The average equalisation efficiency can be improved from 52% to 60% compared with the equaliser operated in CICM. The maximum equalisation efficiency can achieve 61.8% for the designed test sample. It will be significantly improved by using the optimisation designed for passive and active devices, and alternating soft-switching technology in the future study.

Figure 12*a* and *b* shows the experimental cell-voltage trajectories during equalisation for the proposed equalisation scheme without and with FLC-BEC under a floating state that is neither a charged nor a discharged state. After all cell voltages were balanced within the 0.0196 (V), which is the hardware resolution limit of the ADC0804 convertor, the BMS sent a command to cut off the MOSFET and stop the cell-voltage-balance equalisation process. The intelligent equalisation method could balance all adjoining cell voltages in the battery string to the same voltage level. Each cell was simultaneously charged to its end-of-charge voltage. The total charging capacity of the battery string was thereby increased. The proposed equalisation scheme with the designed FLC-BEC, operated in DICM, can shorten the equalisation time by about 30% compared with the proposed equalisation scheme without FLC-BEC.

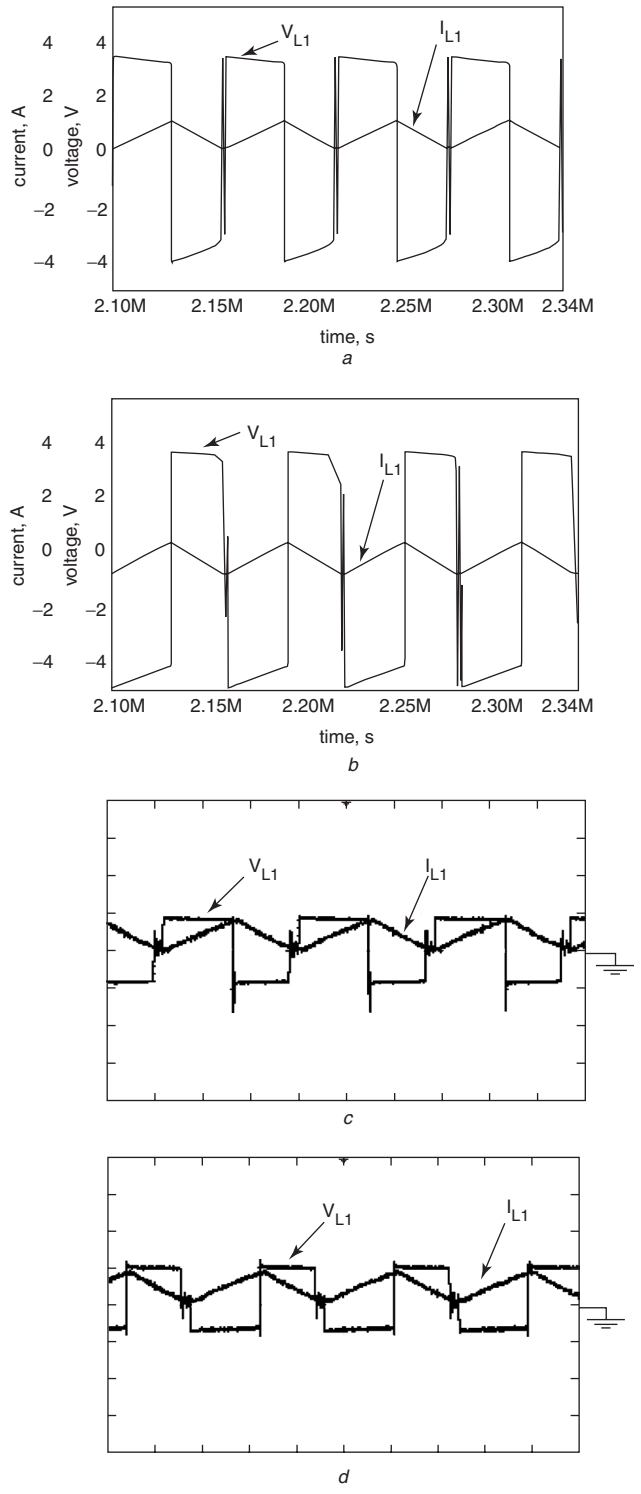

Fig. 9 *Simulations and experimental results of inductor currents and voltages of the proposed equaliser*
a For $V_{B1} > V_{B2} > V_{B3}$
b For $V_{B1} < V_{B2} < V_{B3}$ 5V/division, 20 μs/division
c For $V_{B1} > V_{B2} > V_{B3}$
d For $V_{B1} < V_{B2} < V_{B3}$ 5V/division, 20 μs/division

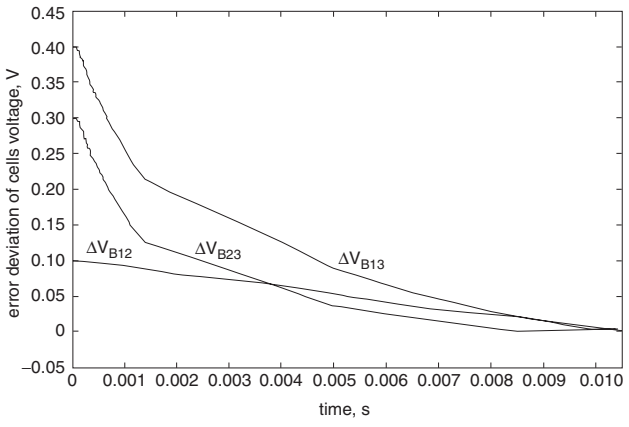

Fig. 10 *Simulation results of the corresponding error deviation of control output cell voltages*

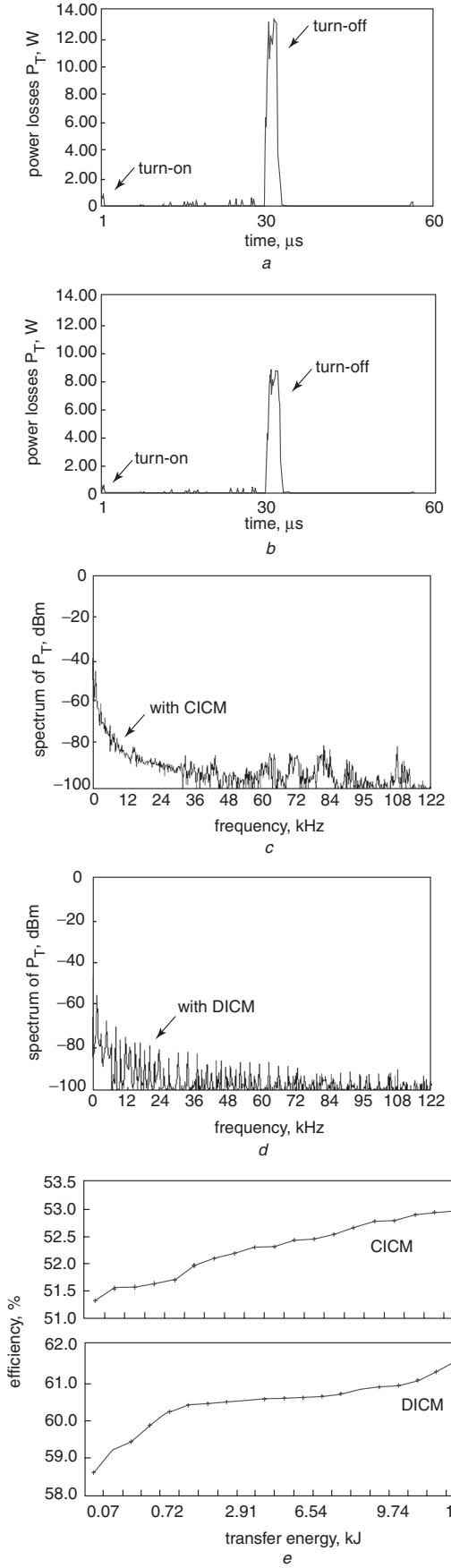

Fig. 11 *Experimental power losses of MOSFET switch*
a CICM
b DICM
c CICM
d DICM
e Equalisation efficiency

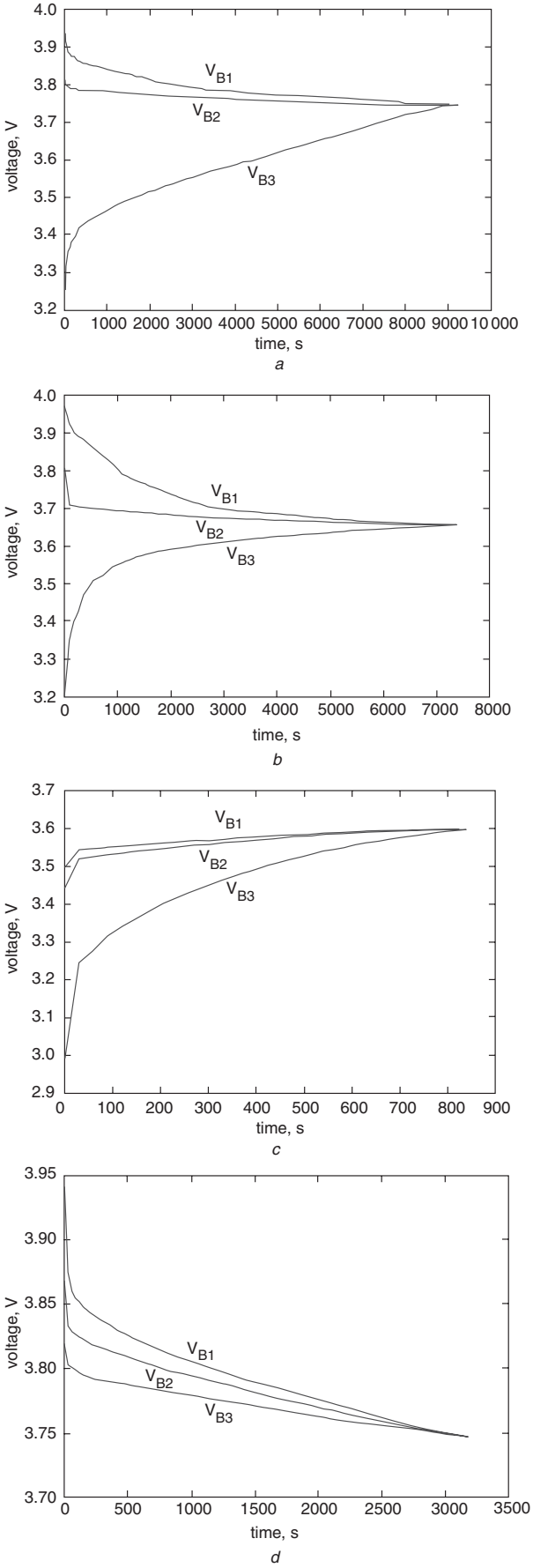

Fig. 12 *Experimental cell-voltage curves for proposed equaliser*
a Floating state without FLC-BEC
b Floating state with FLC-BEC
c Charging state with FLC-BEC
d Discharging state with FLC-BEC

Figure 12*c* and *d* show the voltage trajectories for three cells during equalisation using the proposed equalisation scheme with the designed FLC-BEC under the charge and discharge states, respectively. The charge and discharge currents for the lithium–ion-battery string were set at 1 A. The equalisation performance and equalisation time for the proposed DICM ICEs with FLC-BEC were significantly improved.

In lithium–ion battery-string applications, a single cell failure may result in the whole battery string requiring replacement, a significant cost and maintenance risk of the battery pack [13]. Individual cell equalisation with the proposed fuzzy controller can thus help equalise the string by transferring energy from the strong cell to the rest of the string when desired by the predesigned intelligent controller. To verify the influence of ICE and FLC-BEC on battery-pack performance, an experimental study was conducted to simulate a stationary-battery application. Three strings of three batteries with the three ICEs were assembled with three old MRL/ITRI 10 Ah lithium–ion cells. The three schemes are the system without ICE, with the proposed ICE, and with the proposed ICE and FLC-BEC, respectively. The chosen performance evaluations of the system were installed in the automatic battery-testing system (Arbin Instrument) at Materials Research Laboratories, Industrial Technology Research Institute (MRL, ITRI) with the following simulated charge/discharge cycles:

Step (*i*): Start with a full charge in the cells.

Step (*ii*): The string will be discharged at the C/2 rate until the lowest cell voltage reaches the end-of-discharge voltage (2.8 V/cell).

Step (*iii*): Rest for 20 min.

Step (*iv*): The string will then be recharged at the C/8 rate to the full charge state of the battery string until the highest cell voltage reaches the end-of-charge voltage (4.1 V/cell).

Step (*v*): The cycle will be repeated from steps (ii) to (iv) until the predetermined examination point.

A battery-monitoring system was used to measure and record the individual cell voltages and capacities over time for the three strings during the test. The ambient temperature was set and maintained between 35°C and 43°C. Figure 13*a* shows the cell voltages of the string without ICE during the final stage of the test cycle. The voltages of cells 1 and 3 were greater than that of cell 2. Cell 2 was less efficient at the charge/discharge cycles. The variations in cell voltages at the end-of-charge/discharge states are quite large. The amount of energy output has degraded as one of the old batteries has not been properly charged. The battery string with ICE but without FLC-BEC gave improved voltage performance, as shown in Fig. 13*b*. The ICE functioned as suitable energy-transfer devices to move the energy from the stronger battery into the older cell within the same end-of-charge/discharge state during the testing cycle. This allowed all batteries to be charged/discharged to the maximum/minimum charging/discharging state in the string applications. The cell voltages of the string with ICE and FLC-BEC during the final stage of the testing cycles were showed in Fig. 13*c*. Cell-voltage-variation issues were solved by the battery string with ICE and FLC-BEC, as the equalisers always distributed energy between the individual cells to minimise the load and voltage imbalances, as shown in Fig. 13*b* and *c*. The charged capacities were increased by about 15.1% and

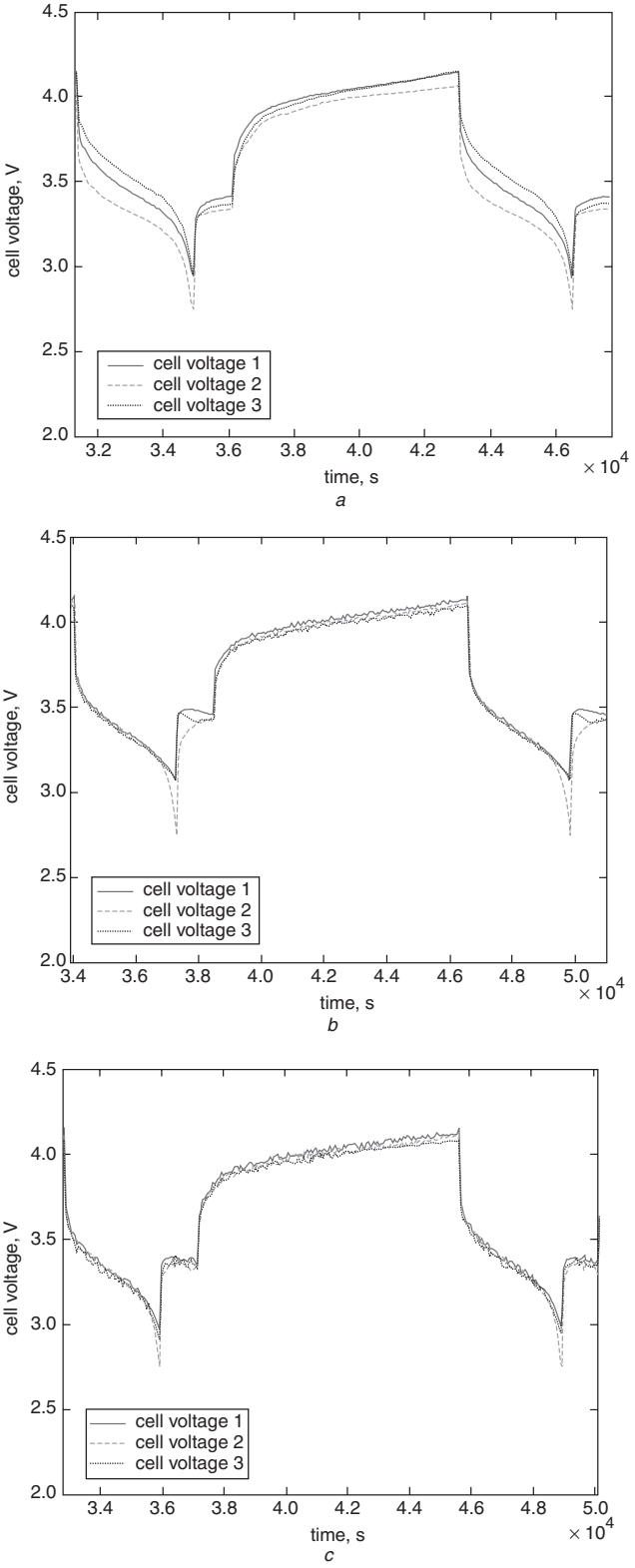

Fig. 13 *Cell voltages during the specified discharge/charge testing cycles in final stage*
a For string without ICE
b For string with ICE but without FLC-BEC
c For string with ICE and FLC-BEC

19.6% for the strings with the proposed ICE and the ICE with FLC-BEC, respectively. The discharged capacity of the string with the proposed ICE and FLC-BEC was increased by about 2% compared with the equaliser without FLC-BEC. The voltage-equalisation performance and equalisation time of the cell voltages improved during the above test

cycle under the same charge/discharge conditions. The FLC can improve the performance of battery equalisation and reduce the equalisation time, as shown in Figs. 12 and 13. It has also been shown in [13] that a well designed ICE can extend the cycle life of the battery. The cycle-life measurement of the battery string with the proposed ICE and FLC-BEC is under study, and the results will be submitted in due course.

The proposed battery-equalisation scheme was designed to operate at DICM. This greatly decreases the MOSFET switching losses in the convertor during the equalisation process. The proposed DICM-designed equaliser with FLC-BEC can shorten the equalisation time and reduce the switching losses; therefore, the equalisation efficiency could be improved compared with the same equalisation scheme without FLC-BEC. Co-ordinated design of the battery-charging algorithm and equalisers, and the quasir-esonant zero-current-switching technology application for reducing the switching losses in the battery equalisation will be suggested for later study [14].

5 Conclusions

The proposed ICE was designed at DICM to reduce the switching losses and increase the equalisation efficiency during the cell-voltage-balancing processing. A systematic designed approach was used to design the FLC-BEC to control the equalisation process and decrease the equalisation time.

In a practical lithium-based battery-pack system design, the effect of cell-imbalance effects in the battery string must be evaluated. These factors must be weighed against the cost of various cell-balancing solutions and the execution time required in the charging process. Using the proposed intelligent equalisation method for a lithium–ion battery string, each cell can be charged/discharged simultaneously to its end-of-charge/discharge voltage. The equalisation time and the total charge/discharge capacity of the battery string will be improved, with guaranteed safe operation.

6 Acknowledgments

This work was financially supported by the National Science Council of Taiwan, under grants NSC 91-2213-E-030-007 and NSC 92-2213-E-030-020. The authors thank MRL/ITRI of Taiwan for supplying lithium–ion batteries and testing, and Dr. Yu-Fu Chou and Bing-Ming Lin, manager of the Division of Energy Storage Materials and Technology, EV Battery Development Project, for their suggestions on this research.

7 References

1 Venkatasetty, H.V., and Jeong, Y.U.: 'Recent advanced in lithium-ion and lithium-polymer batteries'. Proc. Battery Conf. Applications and Advances, 2002, pp. 173–178
2 Kutkut, N.H.: 'A modular nondissipative current diverter for EV battery charge equalization'. Proc. IEEE Power Electronics Specialists Conf., 1998, pp. 686–690
3 Zhang, Z., and CûK, S.: 'A high efficiency 1.8 kW battery equalizer'. Proc. IEEE Power Electronics Specialists Conf., 1993, pp. 221–227
4 Bentley, W.F.: 'Cell balancing considerations for lithium-ion battery systems'. Proc. Battery Conf. Applications and Advances, 1997, pp. 223–226
5 Moore, S.W., Schneider, P.J.: 'A review of cell equalization methods for lithium ion and lithium polymer battery systems'. SAE technical paper series, 2001, pp. 1–5
6 Chatzakis, J., Kalaitzakis, K., Voulgaris, N.C., and Manias, S.N.: 'Designing a new generalized battery management system', *IEEE Trans.*, 2003, **IE-50**, (5), pp. 990–999
7 Hsieh, G.C., Chen, L.R., and Huang, K.S.: 'Fuzzy-controlled li-ion battery charge system with active state-of-charge controller', *IEEE Trans.*, 2001, **IE-48**, (3), pp. 585–593
8 Melin, P., and Castillo, O.: 'Intelligent control of complex electro-chemical system with a neuro-fuzzy-genetic approach', *IEEE Trans.*, 2001, **IE-48**, (5), pp. 951–955
9 Lee, Y.S., and Jao, C.W.: 'Fuzzy controlled lithium-ion battery equalization with state-of-charge estimator'. Proc. IEEE Conf. Systems, Man and Cybernetics, 2003, pp. 4431–4438
10 Maksimovic, D., and CûK, S.: 'A unified analysis of PWM converters in discontinuous modes', *IEEE Trans.*, 1991, **PE-6**, (3), pp. 476–490
11 Trzynadlowski, A.M.: 'Introduction to modern power electronics' (John Wiley & Sons, Inc., 1998), pp. 376–379
12 Driankov, D., Hellendoom, H., and Reinfrank, M.: 'An introduction to fuzzy control' (Springer, 1996, Chap. 6), pp. 245–258
13 Krein, P.T., and Balog, R.: 'Life extension through charge equalization of lead-acid batteries'. Proc. Battery Conf. on Applications and Advances, 2002, paper 32.1, pp. 1–8
14 Lee, Y.S., and Cheng, G.T.: 'ZCS bi-directional DC-to-DC converter application in battery equalization for electric vehicles'. Proc. IEEE Power Electronics Specialists Conf., 2004, pp. 2766–2772